BioSystems 106 (2011) 9–18

Contents lists available at ScienceDirect

BioSystems

journal homepage: www.elsevier.com/locate/biosystems

Bifurcation analysis and effects of changing ionic conductances on pacemaker rhythm in a sinoatrial node cell model

Zhenxing Pan[a,*], Rei Yamaguchi[a], Shinji Doi[b]

[a] Graduate School of Engineering, Osaka University, 2-1 Yamadaoka, Suita, Osaka 565-0871, Japan
[b] Graduate School of Engineering, Kyoto University, Kyotodaigaku-katsura, Nishikyo-ku, Kyoto 615-8510, Japan

ARTICLE INFO

Article history:
Received 7 June 2010
Received in revised form 7 March 2011
Accepted 1 June 2011

Keywords:
Pacemaker rhythm
Sinoatrial node
Ion channel
Yanagihara–Noma–Irisawa model
Bifurcation analysis
Parameter sensitivity

ABSTRACT

The electrical excitation (action potential generation) of sinoatrial node (cardiac pacemaker) cells is directly related to various ion channels (pore-forming proteins) in cell membranes. In order to analyze the relation between action potential generation and ion channels, we use the Yanagihara–Noma–Irisawa (YNI) model of sinoatrial node cells, which is described by the Hodgkin–Huxley-type equations with seven variables. In this paper, we analyze the global bifurcation structure of the YNI model by varying various conductances of ion channels, and examine the effects of these conductance changes on pacemaker rhythm (frequency of action potential generation). The coupling effect on pacemaker rhythm is also examined approximately by applying external current to the YNI model.

1. Introduction

In excitable dynamical systems (such as heart and neurons), pacemakers play an important role in driving the whole systems. Due to the importance, a lot of studies have been done to analyze the impacts of pacemakers on excitable dynamical systems. One of the most interesting impacts may be the pacemaker-driven stochastic resonance on noise-introduced systems (networks) (Perc and Marhl, 2006; Perc, 2007, 2008; Perc and Gosak, 2008; Ozer et al., 2009). With the aid of additive noises, the stochastic resonance occurs and the pacemakers enforce their rhythms on the whole networks. Perc et al. have shown that the correlations between pacemaker rhythms and responses of networks are dependent on noise intensities, coupling strengths and underlying structures of networks (such as small-world network Watts and Strogatz, 1998, scale-free network Barabási and Albert, 1999). Besides the additive noises, the direct inputs into pacemakers will also affect the whole systems since they vary pacemaker rhythms directly. As a basis, some studies have already examined the responses of a pacemaker neuron to various inputs, such as periodic pulse train (Sato et al., 1997), transient pulse train (Yamanobe et al., 1998), stochastic pulse train (Yamanobe and Pakdaman, 2002), spike train (Hasegawa, 2000) and fixed delay stimulation (Gómez et al., 2001). In some ways, there are mutual impacts between pacemakers and their present systems, and the above results for different inputs can partially show the responses of pacemakers to different system impacts (coupling effects). Although the system impacts may disturb the pacemakers, they may also excite some units to become "pacemakers" (Jacquemet, 2006). On the other hand, when the pacemakers try to drive the whole systems, energy consumption is required in the process, thus energy efficiency becomes an evaluation of the actual impacts of pacemakers on the systems. An energy function has been introduced into neuron models to evaluate the energy efficiency among coupled neurons for different coupling types (unidirectional or bidirectional) and different coupling strengths (Torrealdea et al., 2006, 2009). Moreover, since the heart is a typical pacemaker-driven system, some heart-related studies have been done by using oscillator models or statistical models. It has been shown that, the model of two coupled oscillators (pacemakers) can show the dynamics of heartbeat (Di Bernardo et al., 1998) and can reproduce the global features of respiratory sinus arrhythmia (RSA) (Christen et al., 2001), and the point process probability model can be applied to cardiovascular control (Barbieri and Brown, 2008).

Among various pacemakers, sinoatrial node (cardiac pacemaker) has gained widespread attention due to its significant impact on the heart (Brown, 1982; Bowman and Jongsma, 1986; Irisawa et al., 1993). The cardiac pacemaker cells generate electrical signals (action potentials Wahler, 2001) periodically to drive the cardiac activity, and the rhythm (frequency of action potential generation) mainly decides the heart rate. The electrical exci-

* Corresponding author.
E-mail addresses: pan@is.eei.eng.osaka-u.ac.jp (Z. Pan), doi@kuee.kyoto-u.ac.jp (S. Doi).

0303-2647/$ – see front matter © 2011 Elsevier Ireland Ltd. All rights reserved.
doi:10.1016/j.biosystems.2011.06.001

tation (action potential generation) of cardiac pacemaker cells is directly related to various ion channels (pore-forming proteins) in cell membranes. When the ion channels open, specific ions pass through them, and the membrane potential (electrical potential difference between the inside and the outside of cell membrane) changes. As a result, the action potentials are generated (Wahler, 2001). The cells themselves have an amazing autonomic function, and their studies are essential for analyzing the whole cardiac pacemaker. In order to study the mechanism of cardiac pacemaker cells, not only physiological experiments but also mathematical models (which describe the relation between membrane potential and ion channels or currents in cells) are used (Wilders, 2007; Noble, 2002).

Start with the Yanagihara–Noma–Irisawa (YNI) model (Yanagihara et al., 1980), various cardiac pacemaker cell models have been proposed. With the development of measurement technique and accumulation of experimental data, cell models become detailed and complicated to simulate the action potential generation suitably (Wilders, 2007; Fink et al., 2011). For examples, Irisawa and Noma (1982) made an extension of the YNI model by incorporating some new experimental data. Noble and Noble (1984) developed a new sinoatrial node cell model from a Purkinje fiber model (DiFrancesco and Noble, 1985), which firstly incorporated the sodium–calcium exchanger and sodium–potassium pump. Then the model of Noble and Noble (1984) was extended by Wilders et al. (1991), and the model of Wilders et al. (1991) was again extended by Dokos et al. (1996). Zhang et al. (2000) considered the regional difference of sinoatrial node and proposed two types of cell models (peripheral and central cell models). The recent models have become very complicated such as those proposed by Kurata et al. (2002) and Sarai et al. (2003).

Most of these cell models are the Hodgkin–Huxley-type (HH-type) models. The HH-type models are based on the famous Hodgkin–Huxley model of a squid nerve, which is described by nonlinear ordinary differential equations with four variables (Hodgkin and Huxley, 1952). The analysis of cell models provides us with very useful information on cellular activity besides physiological experiments. However, since these cell models are high-dimensional, the analysis of them is very difficult, especially for the detailed models. In this paper, we use the rather classical YNI model since it is a typical sinoatrial node cell model and still possesses the essential features of cardiac pacemaker cells in spite of its simplicity (Keener and Sneyd, 2008).

Since the HH-type models are described by nonlinear ordinary differential equations, their dynamics may qualitatively change when varying their parameters (Doi et al., 2010). Such a qualitative and critical change of dynamics is called a bifurcation (Guckenheimer and Holmes, 2002). So far, it has been shown that, the bifurcation analysis of various cardiac cell models (particularly models of ventricular myocardial cells) is helpful in understanding the dependence of the dynamics of cardiac cells on various parameters (Nagata et al., 2006; Takahashi et al., 2006; Yamaguchi et al., 2007, 2008).

In this paper, we analyze the global bifurcation structure of the YNI model by varying various conductances of ion channels as bifurcation parameters. Based on the bifurcation structure, we examine the relations between ion channels (currents) and pacemaker rhythm, and also examine the interrelations between two ion currents. The obtained parameter sensitivities are used to compare the effects of various ion currents on pacemaker rhythm. Moreover, we examine the coupling effect on pacemaker rhythm approximately by applying external current to the YNI model. The results partially show the difference of pacemaker rhythm between a single cell and coupled cells, and provide us much more information about the whole cardiac pacemaker.

2. Yanagihara–Noma–Irisawa Model

The YNI model is described by the HH-type equations with seven variables: membrane potential V (mV), gating variables m, h, d, f, q, p (dimensionless). The temporal variation of membrane potential V is described by

$$\frac{dV}{dt} = -\frac{1}{C}(I_{Na} + I_s + I_h + I_K + I_l - I_{ext}) \tag{1}$$

where C (= 1 μF/cm^2) and I_{ext} (μA/cm^2) denote the membrane capacitance and the external current, respectively. In general, the sinoatrial node cells couple with each other by gap junction channels, and exchange ions via these channels (Anumonwo et al., 1992; Verheule et al., 2001). The coupling current between two coupled cells is dependent on the difference of their membrane potentials and the conductance of gap junction channel (Van Rijen et al., 1998; Joyner et al., 2006). For simplicity, we use the external current I_{ext} as the coupling current to analyze coupling effect approximately. I_{Na}, I_s, I_h, I_K and I_l (μA/cm^2) denote the sodium current, the slow inward current, the hyperpolarization-activated current, the potassium current and the leak current, respectively. These ion currents are described by

$$I_{Na} = c_{Na} G_{Na} m^3 h (V - 30), \quad G_{Na} = 0.5 \tag{2}$$

$$I_s = c_s G_s (0.95d + 0.05)(0.95f + 0.05)\left(\exp\left(\frac{V - 30}{15}\right) - 1\right), \quad G_s = 12.5 \tag{3}$$

$$I_h = c_h G_h q (V + 25), \quad G_h = 0.4 \tag{4}$$

$$I_K = c_K G_K p \frac{\exp(0.0277(V + 90)) - 1}{\exp(0.0277(V + 40))}, \quad G_K = 0.7 \tag{5}$$

$$I_l = c_l G_l \left(1 - \exp\left(-\frac{V + 60}{20}\right)\right), \quad G_l = 0.8 \tag{6}$$

where G_{ion} (ion = Na, s, h, K, l) (mS/cm^2) are the maximum conductances of ion channels. The parameters c_{ion} (dimensionless) are the newly introduced coefficients in order to examine the effects of changing the conductances of ion channels, and their standard values are 1.0. The gating variables m, h, d, f, q, p (ranging between 0 and 1) denote the effects of opening and closing of ion channels. Temporal variations of these gating variables are described by

$$\frac{dx}{dt} = \alpha_x(V)(1 - x) - \beta_x(V)x, \quad (x = m, h, d, f, q, p) \tag{7}$$

where $\alpha_x(V)$ and $\beta_x(V)$ (ms^{-1}) are the (voltage-dependent) rate constants of the transition between open and closed states of gates. The details are listed in Appendix A.

The YNI model can simulate the typical action potentials of sinoatrial node cells very well. Fig. 1(a) and (b) shows temporal variations of membrane potential and ion currents in normal condition (I_{ext} = 0.0 μA/cm^2, c_{ion} = 1.0), respectively. The YNI model is a sinoatrial node cell model of rabbit, and the normal period of action potential generation is about 380 ms (In general, the normal period of rabbit is in the range of 185–462 ms (Anon., 2007).) Since the sinoatrial node plays the role of cardiac pacemaker, sinoatrial node cells generate periodic action potentials spontaneously without external electrical stimuli (I_{ext} = 0.0 μA/cm^2). The inward currents flowing from the outside into the inside of cell membrane (denoted by negative values in Fig. 1(b)) and outward currents (positive values) cause the membrane potential to increase (depolarization) and decrease (repolarization), respectively. In the five ion currents, the slow inward current I_s has the largest amplitude, and the hyperpolarization-activated current I_h has the least one in the normal action potential generation process.

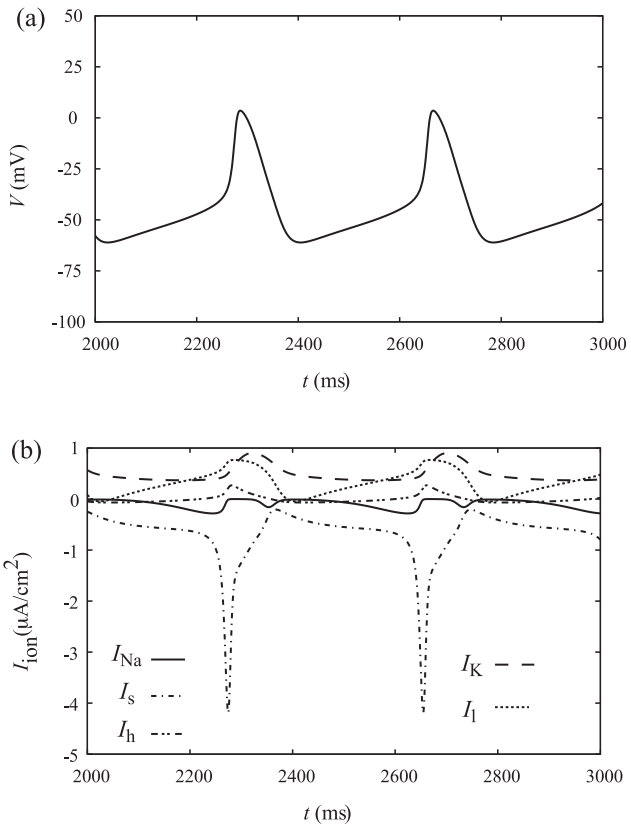

Fig. 1. Temporal variations of (a) membrane potential V and (b) ion currents I_{ion} (ion = Na, s, h, K, l) in normal condition (I_{ext} = 0.0 μA/cm^2, c_{ion} = 1.0). In the panel (b), the inward currents (flowing from the outside into the inside of cell membrane) and outward currents are denoted by negative and positive values, respectively.

3. Effects of Changing Conductances of Ion Currents on Pacemaker Rhythm

The sinoatrial node is made up of thousands of cells and electrical currents are propagated among them. In this section, we ignore the electrical currents (I_{ext} = 0.0 μA/cm^2), and analyze the effects of changing conductances of ion currents on pacemaker rhythm of a single cell.

This paper uses the bifurcation analysis software AUTO (Doedel et al., 1997) to analyze the YNI model, where the conductance coefficients c_{ion} are varied as bifurcation parameters. Although the membrane potential V is a function of time, here we only investigate its characteristics in steady states (equilibrium values, (local) maximum and minimum values, periods).

3.1. The Sodium Current I_{Na}

The one-parameter bifurcation diagram of the YNI model, where the bifurcation parameter is the conductance coefficient c_{Na}, is shown in Fig. 2(a), in which the value of V in the steady state is plotted for each value of c_{Na}. (Under physiological conditions, the conductance of each ion channel would not be negative or too large. However, in order to show the global bifurcation structure of the model, we compute for negative or very large conductance coefficients if necessary.) The solid and broken curves show stable and unstable equilibrium points, respectively. The symbols • and ○ show the maximum values of V of stable and unstable periodic orbits, respectively. The bifurcation points of Hopf, saddle-node, double-cycle, period-doubling and homoclinic bifurcations (Guckenheimer and Holmes, 2002) are denoted by HB, SN, DC, PD and HC (with a number), respectively. The values of (c_{Na}, V) at these bifurcation points are as follows. HB1: (4.55, −29.7); HB2: (0.287, −44.7); SN1: (0.000964, −36.5); SN2: (0.358, −42.6); DC1: (3.84, −9.71); DC2: (3.92, −2.00); PD1: (3.91, −1.10); PD2: (3.67, 2.83); PD3: (0.255, 2.63); HC1: (0.254, −1.54); HC2: (0.258, −40.1).

At the Hopf bifurcation (HB), the stability of an equilibrium point changes, and a (stable or unstable) periodic orbit is bifurcated. At the saddle-node bifurcation (SN), a pair of equilibrium points are generated or disappear. The double-cycle bifurcation (DC) is the same as the saddle-node bifurcation of periodic orbits, and a pair of periodic orbits are generated at the bifurcation point. At the period-doubling bifurcation (PD), the stability of periodic orbit changes, and another periodic orbit with a double period is generated. The homoclinic bifurcation (HC) is a special bifurcation, and a periodic orbit collides with an equilibrium point. Near the homoclinic bifurcation, the period of periodic orbit becomes very long.

For each value of c_{Na} between the two Hopf bifurcation points HB1 and HB2, a (stable or unstable) periodic orbit exists. Periods of periodic orbits are also shown in the diagram. In normal condition (c_{Na} = 1.0), a stable periodic orbit whose period is about 380 ms exists, and Fig. 2(d) shows the corresponding waveform of membrane potential. The period of periodic orbit varies much when changing c_{Na}, whereas the amplitude varies little. It shows that, the conductance change has a strong effect on the pacemaker rhythm, but it has a weak effect on the intensity of action potential generation. The period decreases when c_{Na} is increased. Fig. 2(c) and (e) shows two typical waveforms of membrane potentials, whose periods are long and short, respectively. In Fig. 2(a), the variation of period is little when c_{Na} is increased from 1.0 (normal value), whereas it is big when c_{Na} is decreased from 1.0. Especially when c_{Na} takes a value near 0.25, the period changes much sensitively to c_{Na}. This sensitivity is mainly caused by the homoclinic bifurcation HC1 (and the two saddle-node bifurcations SN1 and SN2). These results show that the parameter sensitivity of pacemaker rhythm in the case of a small value of c_{Na} is stronger than that in the case of a large value of c_{Na}.

In both the left side of HB2 and the right side of HB1, only equilibrium points exist. Because of the abnormality of Na^+ channel there (c_{Na} is too small or too large), it is difficult to generate action potentials periodically and continuously. The typical waveforms of membrane potentials in the two cases are shown in Fig. 2(b) and (f), respectively. Both of the membrane potentials asymptotically converge to the stable equilibrium points, but the values of equilibrium points are different in the two cases.

Since only unstable periodic orbits and unstable equilibrium points were detected by AUTO for the values of c_{Na} between PD2 and DC1 in Fig. 2(a), we also computed the one-parameter bifurcation diagram by numerical simulations for $3.6 \le c_{Na} \le 4.0$ (Fig. 3(a)). In this diagram, both the local maximum and minimum values of V for each value of c_{Na} were plotted. When c_{Na} is increased from the period-doubling bifurcation point PD2 to the double-cycle bifurcation point DC1, many other bifurcations and possibly chaotic solutions are generated sensitively to the conductance of Na^+ channel. The waveforms of membrane potentials when c_{Na} = 3.7 and 3.8 are shown in Fig. 3(b) and (c), respectively. Both waveforms show abnormalities in action potential generation.

3.2. Comparison of Effects of Various Ion Currents on Pacemaker Rhythm

Fig. 4 compares the effects of various ion currents on pacemaker rhythm, in which the periods of stable periodic orbits are plotted when each conductance coefficient c_{ion} is varied. As for the ion current I_h, the variation of c_h does not change the period much, which means that the parameter sensitivity of pacemaker rhythm as for I_h is very weak. For other four ion currents, the period signif-

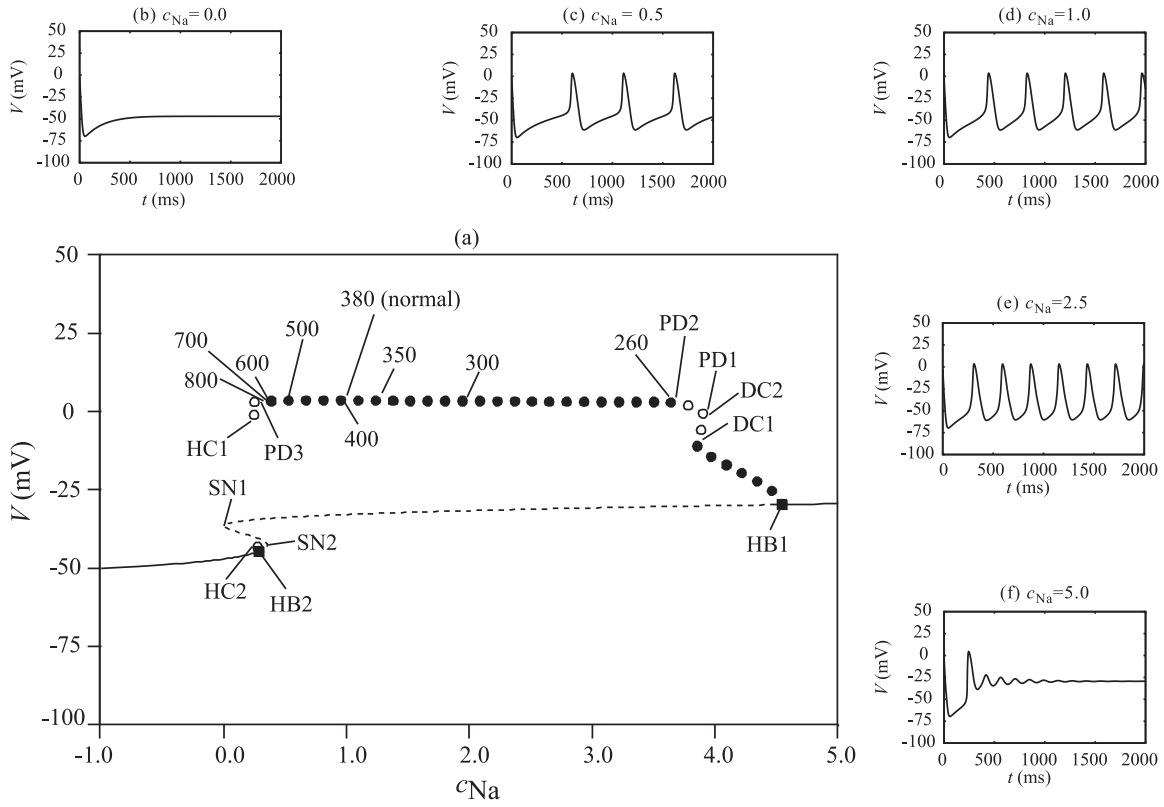

Fig. 2. (a) One-parameter bifurcation diagram as for the bifurcation parameter c_{Na} obtained by AUTO (Doedel et al., 1997), in which the value of membrane potential V in the steady state is plotted for each value of c_{Na}. The solid and broken curves show stable and unstable equilibrium points, respectively. The symbols • and ◦ show the maximum values of V of stable and unstable periodic orbits, respectively. The bifurcation points of Hopf, saddle-node, double-cycle, period-doubling and homoclinic bifurcations (Guckenheimer and Holmes, 2002) are denoted by HB, SN, DC, PD and HC (with a number), respectively. The values on some stable periodic orbits show their periods (ms) and "normal" denotes the period 380 ms in normal condition (c_{Na} = 1.0). (b)–(f) Typical waveforms of membrane potentials for various values of c_{Na}.

icantly changes with the variation of each conductance coefficient, particularly in the range of long period. Moreover, for the inward currents I_{Na} and I_s, the period decreases when c_{Na} or c_s increases. For the outward currents I_K and I_l, the period increases when c_K or c_l increases. These results show that the parameter sensitivities of pacemaker rhythm as for the above four ion currents are very high.

4. Interrelations between Two Ion Currents

In the above section, we have analyzed the parameter sensitivity of pacemaker rhythm as for each ion current (channel) solely. In this section, we analyze the parameter sensitivity on two ion currents simultaneously. The bifurcation points shown in the one-parameter bifurcation diagrams may change when another

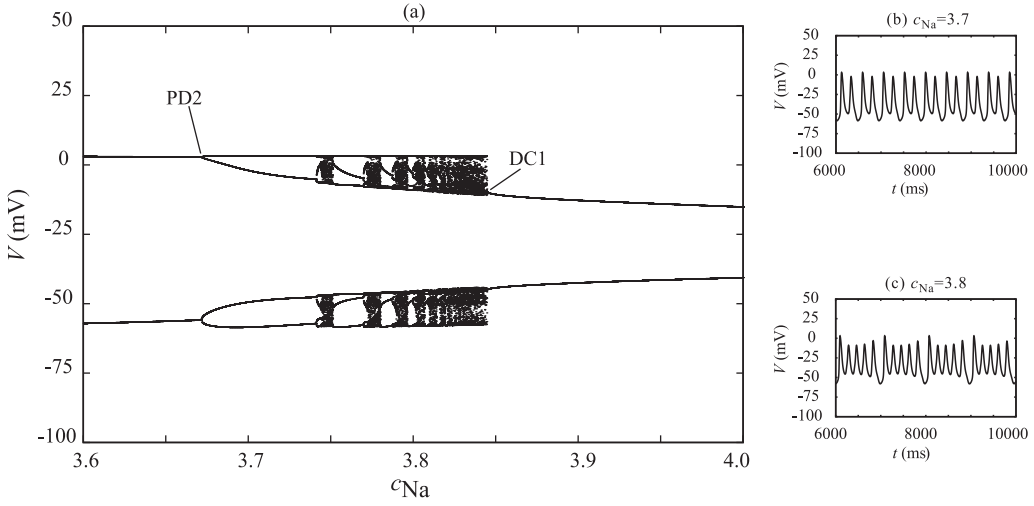

Fig. 3. (a) One-parameter bifurcation diagram as for the bifurcation parameter c_{Na} obtained by numerical simulations, in which both the local maximum and minimum values of membrane potential V are plotted for each value of c_{Na}. The bifurcation points of double-cycle and period-doubling are denoted by DC and PD (with a number), respectively. (b) and (c) Typical waveforms of membrane potentials for two values of c_{Na}.

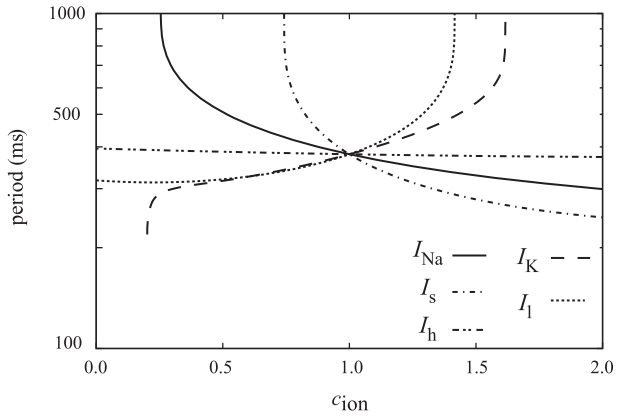

Fig. 4. The periods of stable periodic orbits are plotted when each conductance coefficient c_{ion} (ion = Na, s, h, K, l) is varied, for comparison of the effects of various ion currents on pacemaker rhythm.

conductance coefficient is also varied, and a two-parameter bifurcation diagram shows the loci of various bifurcation points (bifurcation curves) when two conductance coefficients are varied. The contour lines of various periods of stable periodic orbits are also plotted in the diagram to examine the pacemaker rhythm.

4.1. The Sodium Current I_{Na} and the Potassium Current I_K

The two-parameter bifurcation diagram as for the two bifurcation parameters c_{Na} and c_{K} is shown in Fig. 5(a). The curve labeled with "normal" denotes the contour line of period 380 ms, and the point labeled with "BT" denotes the Bogdanov–Takens bifurcation point. This BT point is a special and degenerate bifurcation point where three bifurcation curves of HB, SN and HC meet together. The double-cycle bifurcation curve DC3 meets the Hopf bifurcation curve HB1 at the nHB point which is called a neutral or degenerate Hopf bifurcation point. The values of $(c_{\mathrm{Na}}, c_{\mathrm{K}})$ at these bifurcation points are as follows. BT: (−0.982, 0.117); nHB: (2.62, 0.475). When

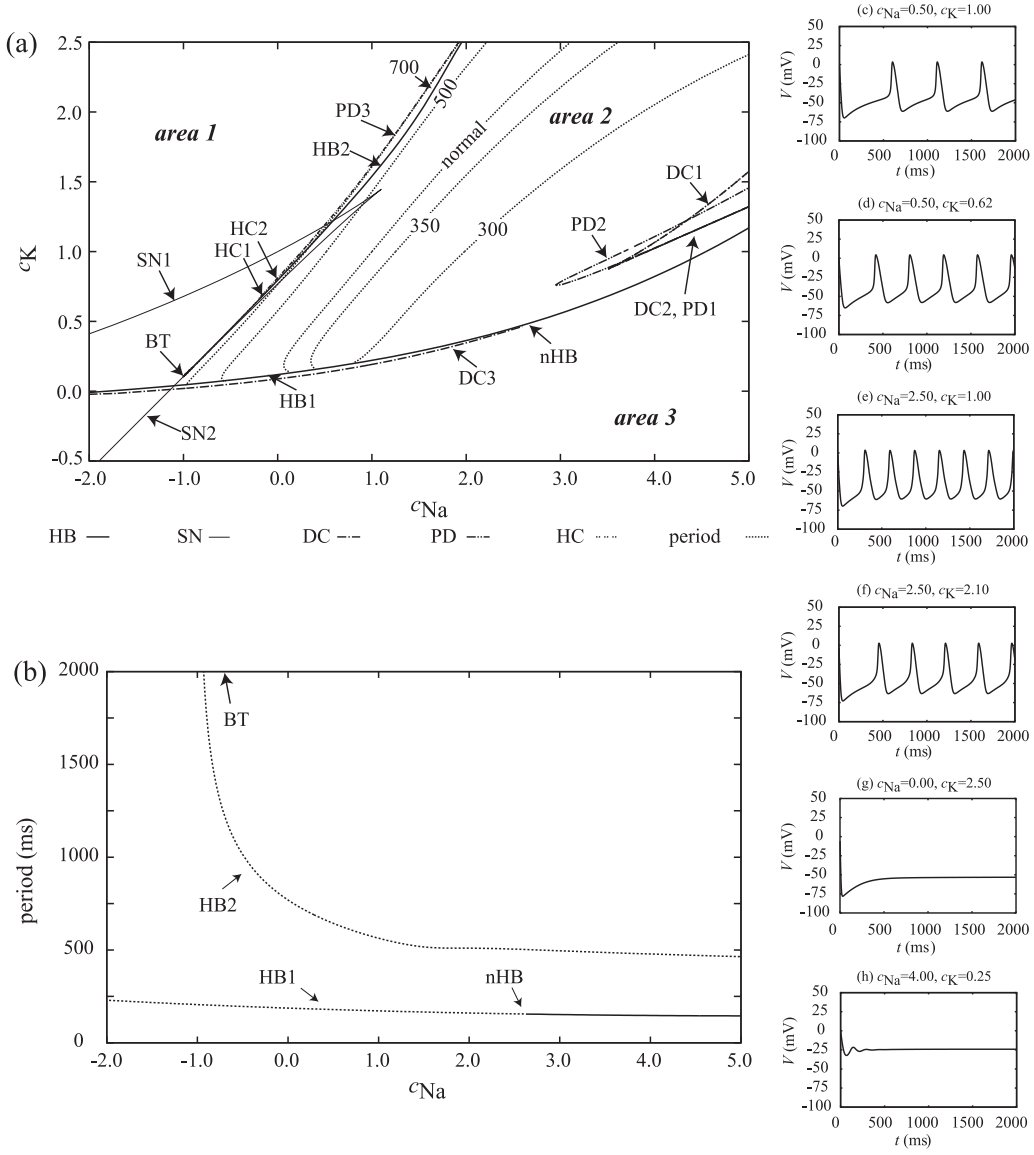

Fig. 5. (a) Two-parameter bifurcation diagram as for the two bifurcation parameters c_{Na} and c_{K}, in which the loci of various bifurcation points (bifurcation curves) and the contour lines of various periods of stable periodic orbits are plotted when c_{Na} and c_{K} are varied. The bifurcation points of Hopf, saddle-node, double-cycle, period-doubling, homoclinic, Bogdanov–Takens, and neutral (degenerate) Hopf bifurcations are denoted by HB, SN, DC, PD, HC, BT, and nHB (with a number), respectively. The values on contour lines show their periods (ms) and "normal" denotes the period 380 ms in normal condition. The bifurcation curves HB1 and HB2 separate the diagram into three areas. (b) Periods of periodic orbits along the Hopf bifurcation curves HB1 and HB2 of (a). (c)–(h) Typical waveforms of membrane potentials for various values of c_{Na} and c_{K}.

c_K is fixed to 1.0 and c_{Na} is varied, the result corresponds to the "one-parameter" bifurcation diagram of Fig. 2(a).

The bifurcation curves HB1 and HB2 separate Fig. 5(a) into three areas. In area 2, various periodic orbits exist. The period becomes short when c_{Na} is increased, and it becomes long when c_K is increased. The density of contour line of long period is high, and that of short period is low (note that near the Hopf bifurcation curve HB2, the contour lines with long period and other bifurcation curves such as HC1 and HC2 gather together). This shows that the parameter sensitivity in the case of long period is stronger than that of short period. Fig. 5(c) and (e) shows two abnormal (too-long and too-short periods) waveforms of membrane potentials when c_{Na} take a small and a large value (c_K is fixed to 1.0), respectively. If we want to get the normal period 380 ms in such abnormal cases of c_{Na}, the value of c_K should be adjusted as shown in Fig. 5(d) and (f). Namely, when two ion currents have a strong interrelation, we can correct the pacemaker rhythm caused by one abnormal ion channel conductance, by adjusting another ion channel conductance.

Fig. 5(g) and (h) shows the typical waveforms in area 1 and area 3, respectively. Both of the membrane potentials converge to the equilibrium points eventually and cannot produce repetitive action potentials.

Fig. 5(b) shows the periods of periodic orbits (stable or unstable) as a function of c_{Na} along the Hopf bifurcation curves HB1 and HB2 of Fig. 5(a). The solid and broken curves correspond to stable and unstable periodic orbits (will be bifurcated from the Hopf bifurcation) respectively, and the stability changes at the neutral (degenerate) Hopf bifurcation point nHB. It shows that the period of periodic orbit varies drastically near the Bogdanov–Takens bifurcation point BT, and the parameter sensitivity of pacemaker rhythm becomes high.

4.2. The Slow Inward Current I_s and the Potassium Current I_K

The two-parameter bifurcation diagram as for the two parameters c_s and c_K is shown in Fig. 6(a). The values of (c_s, c_K) at these bifurcation points are as follows. nHB1: (0.753, 0.0927); nHB2: (0.320, −0.0225). The result of Fig. 6(a) is very similar to that of Fig. 5(a). That is, the repetitive action potentials can be generated in area 2 (which is surrounded by the Hopf bifurcation curves HB1 and HB2), whereas those cannot be generated in area 1 and area 3. For periodic orbits (pacemaker activities) in area 2, the adjustment of c_K (c_s) can recover the abnormal periods caused by c_s (c_K) to the normal period referring to the "normal" contour line.

The variation of period along the Hopf bifurcation curves HB1 and HB2 of Fig. 6(a) is shown in Fig. 6(b). Between the neutral Hopf bifurcation points nHB1 and nHB2, stable periodic orbits are bifurcated from the Hopf bifurcation curve HB1 and HB2. It is obvious that for small values of both c_s and c_K, the period of periodic orbit at Hopf bifurcation varies drastically, and the parameter sensitivities of pacemaker rhythm are very high (please compare the loci of two points nHB1 and nHB2 between panels (a) and (b)).

4.3. The Sodium Current I_{Na} and the Hyperpolarization-activated Current I_h

Fig. 7(a) is the two-parameter bifurcation diagram where c_{Na} and c_h are bifurcation parameters. Both the bifurcation curves and contour lines are almost vertical, which means that the change of c_h does not affect the pacemaker rhythm whereas c_{Na} does affect it much, although the effect of c_h becomes relatively larger when c_{Na} is large. From the waveforms shown in Fig. 7(b)–(d), we can also see that the pacemaker rhythm changes greatly when c_{Na} is varied, but it changes little when c_h is varied. We have also examined other two-parameter bifurcation diagrams as for the parameters: c_h and c_s, c_h and c_K, c_h and c_l, which are not shown in this paper. All results

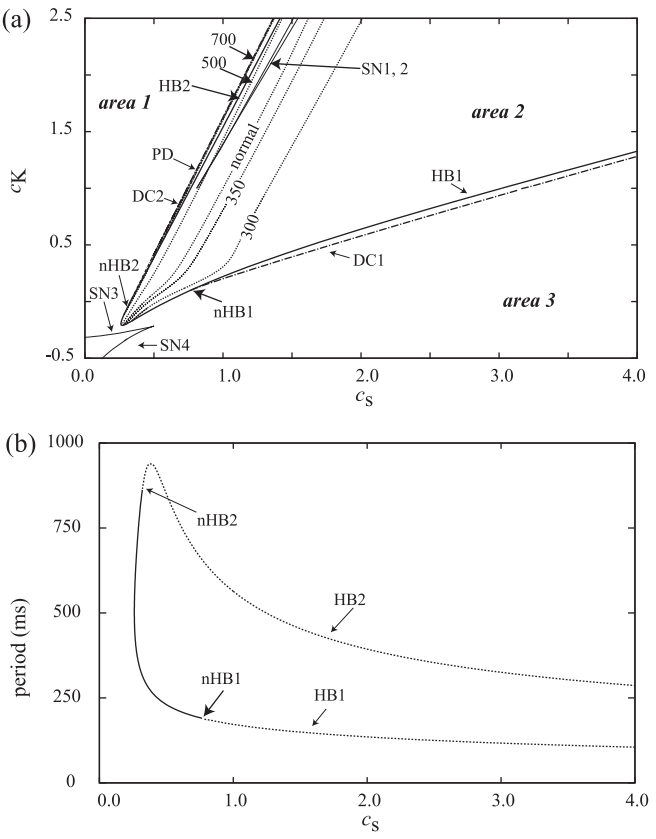

Fig. 6. (a) Two-parameter bifurcation diagram as for the two bifurcation parameters c_s and c_K. The bifurcation points of Hopf, saddle-node, double-cycle, period-doubling, and neutral (degenerate) Hopf bifurcations are denoted by HB, SN, DC, PD, and nHB (with a number), respectively. The values on contour lines show their periods (ms) and "normal" denotes the period 380 ms in normal condition. The bifurcation curves HB1 and HB2 separate the diagram into three areas. (b) Periods of periodic orbits along the Hopf bifurcation curves HB1 and HB2 of (a).

are similar to Fig. 7: I_h has little effect on the period of periodic orbit, and the corresponding ion channel plays a minor role in rhythmic action potential generation.

5. Effect of Changing External Current on Pacemaker Rhythm

So far, we have only examined the pacemaker rhythm of a single cell. In order to examine the pacemaker activity of sinoatrial node, it is necessary to analyze a large number of coupled cells (Joyner et al., 2006). Since it is difficult to analyze such a huge system of many cells, we apply a constant current I_{ext} to the YNI model in order to take into account the coupling effect approximately, and examine the effects of external stimuli on pacemaker rhythm.

At first, we examine the one-parameter bifurcation diagram as for the external current I_{ext} (Fig. 8). The values of (I_{ext}, V) at these bifurcation points are as follows. HB1: (0.802, −26.1); HB2: (−0.180, −45.8); SN1: (−0.201, −37.4); SN2: (−0.157, −42.7); DC: (0.903, −6.34); PD: (−0.194, 1.61); HC1: (−0.195, −1.91); HC2: (−0.194, −38.6). The bifurcation structure of the YNI model shown in Fig. 8 is very similar to that shown in Fig. 2(a), since the positive current I_{ext} can be thought to be an inward current, which plays a similar role to I_{Na} in action potential generation. The periods of periodic orbits between HB1 and HB2 decrease when I_{ext} is increased. It is shown that the external stimuli (positive currents) accelerate action potential generation in cardiac pacemaker cells.

Next, the relations between each ion current and the external current are illustrated in the two-parameter bifurcation diagrams

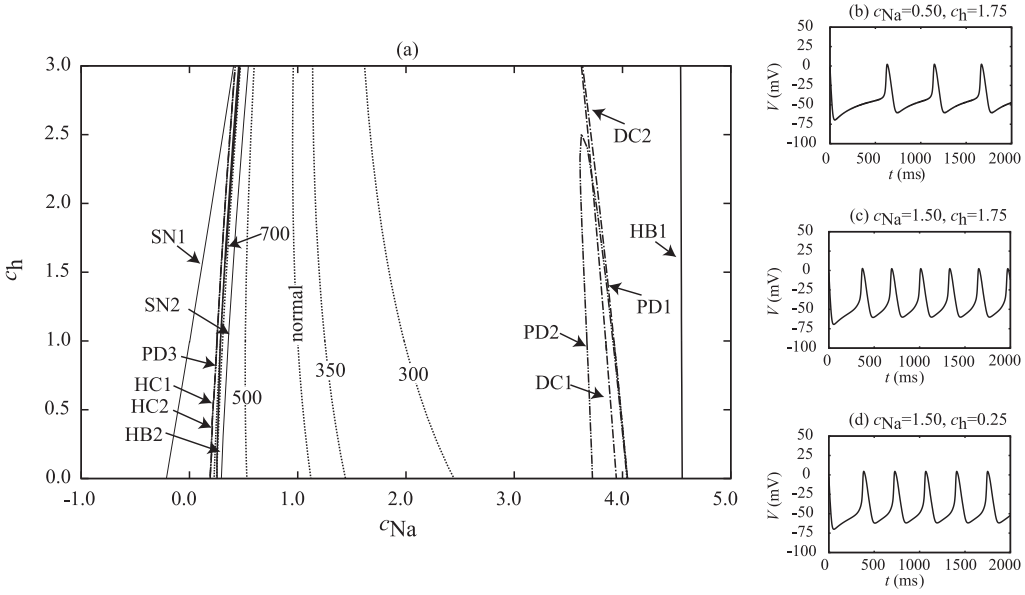

Fig. 7. (a) Two-parameter bifurcation diagram as for the two bifurcation parameters c_{Na} and c_h. The bifurcation points of Hopf, saddle-node, double-cycle, period-doubling and homoclinic denoted by HB, SN, DC, PD and HC (with a number), respectively. The values on contour lines show their periods (ms) and "normal" denotes the period 380 ms in normal condition. (b)–(d) Typical waveforms of membrane potentials for various values of c_{Na} and c_h.

in Figs.9 and 10. Fig. 9(a): the value of (c_{Na}, I_{ext}) at nHB point is (2.962, 0.424); Fig. 9(b): the values of (c_s, I_{ext}) at nHB1 point is (0.612, 0.874) and at nHB2 point is (0.333, 0.466); Fig. 10(a): the value of (c_K, I_{ext}) at nHB point in is (0.0143, −0.225); Fig. 10(b): the values of (c_h, I_{ext}) at nHB point is (7.682, 0.876), and at BT point is (−0.471, 0.175). There are strong interrelations between I_{Na} and I_{ext}, I_s and I_{ext}, I_K and I_{ext}, whereas there is a weak interrelation between I_h and I_{ext}. For the inward currents I_{Na} and I_s, the Hopf bifurcation points HB1 and HB2 shift to left when I_{ext} is increased, which means that a small I_{Na} or I_s can generate repetitive action potentials successfully with the help of I_{ext}. However, the effects of I_{ext} on pacemaker rhythm are different for the above two inward currents. When I_{ext} takes a value near 1.0 μA/cm^2, repetitive action potentials can be generated by adjusting c_{Na}, whereas it cannot be done by adjusting c_s. For the outward current I_K, when I_{ext} is increased, the Hopf bifurcation points HB1 and HB2 shift to right (the opposite direction to the inward currents), and the two points HB1 and HB2 deviate each other. For I_h, both the bifurcation curves and contour lines are almost horizontal, which shows that I_h has little effect on pacemaker rhythm. From the above results, we know that the ion channels of I_{Na}, I_s and I_K play important roles in action potential generation, whereas the ion

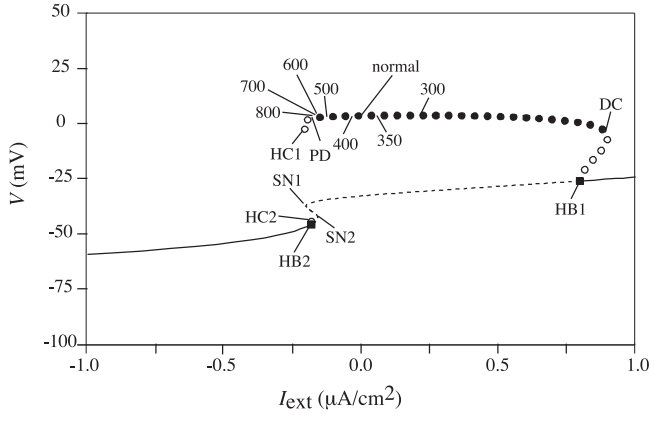

Fig. 8. One-parameter bifurcation diagram as for the bifurcation parameter I_{ext}. The solid and broken curves show stable and unstable equilibrium points, respectively. The symbols • and ◦ show the maximum values of V of stable and unstable periodic orbits, respectively. The bifurcation points of Hopf, saddle-node, double-cycle, period-doubling and homoclinic bifurcations are denoted by HB, SN, DC, PD and HC (with a number), respectively. The values on some stable periodic orbits show their periods (ms) and "normal" denotes the period 380 ms in normal condition.

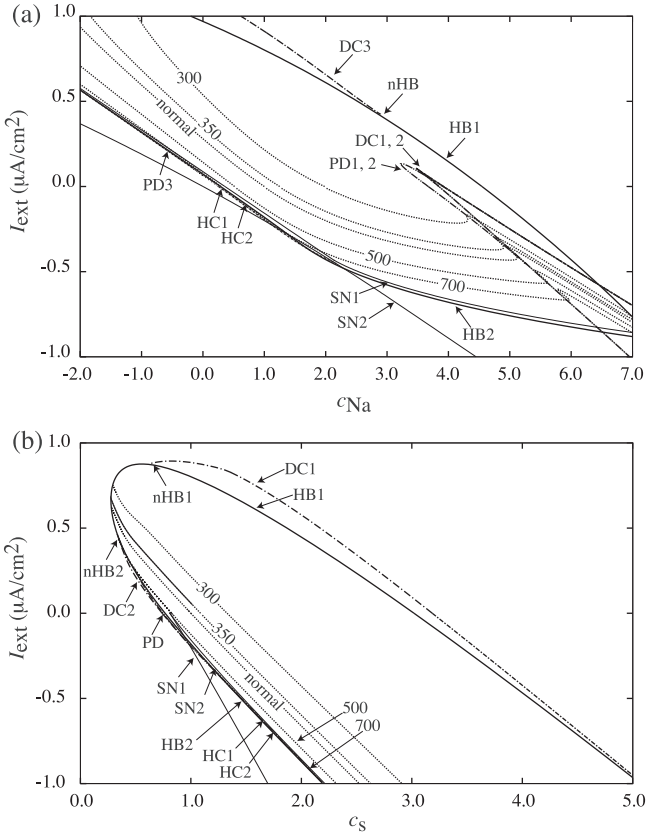

Fig. 9. Two-parameter bifurcation diagram as for the two bifurcation parameters c_{ion} (ion = Na, s) and I_{ext}. The bifurcation points of Hopf, saddle-node, double-cycle, period-doubling, homoclinic and neutral (degenerate) Hopf bifurcations are denoted by HB, SN, DC, PD, HC and nHB (with a number), respectively. The values on some stable periodic orbits show their periods (ms) and "normal" denotes the period 380 ms in normal condition.

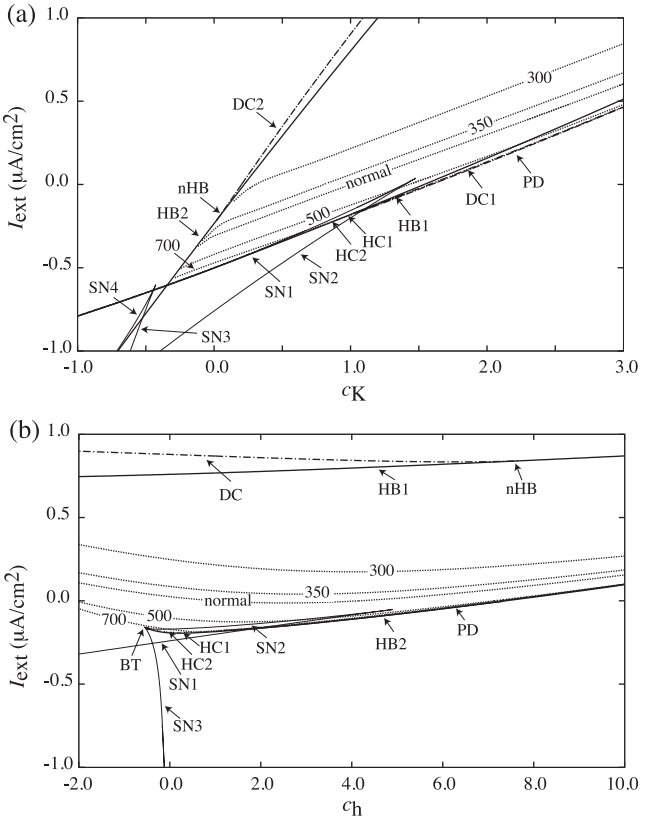

Fig. 10. Two-parameter bifurcation diagram as for the two bifurcation parameters c_{ion} (ion = K, h) and I_{ext}. The bifurcation points of Hopf, saddle-node, double-cycle, period-doubling, homoclinic, Bogdanov–Takens and neutral (degenerate) Hopf bifurcations are denoted by HB, SN, DC, PD, HC, BT and nHB (with a number), respectively. The values on some stable periodic orbits show their periods (ms) and "normal" denotes the period 380 ms in normal condition.

channel of I_h plays a minor role in both a single cell and coupled cells.

6. Conclusion

Focusing mainly on the rhythmic action potential generation (electrical excitation), we have analyzed the global bifurcation structure of the YNI model as a typical cardiac pacemaker cell model. Based on the bifurcation structure, the effects of changing channel conductances and external current on pacemaker rhythm have been examined.

The YNI model considers five ion currents I_{Na}, I_s, I_h, I_K and I_l. At first, we examined the one-parameter bifurcation diagrams as for each conductance coefficient c_{ion}, to analyze the parameter sensitivity of pacemaker rhythm. For I_{Na} and I_s, the increase of conductance decreases the period of action potential generation. For I_K and I_l, the increase of conductance increases the period. These results show that the parameter sensitivities of pacemaker rhythm as for the above four ion currents are high. For I_h, the period changes little when its conductance is varied; its parameter sensitivity is low.

Next, two conductance coefficients were varied simultaneously in the two-parameter bifurcation diagrams, to analyze the interrelations of two ion currents. There are strong relations between I_{Na} and I_K, I_s and I_K, and a weak one between I_{Na} and I_h (since I_h affects the pacemaker rhythm little). We can adjust one ion current to correct the abnormal pacemaker rhythm caused by another ion current when the two ion currents have a strong interrelation.

Moreover, we applied constant external current I_{ext} to the YNI model, and analyzed the coupling effect on pacemaker rhythm approximately. The one-parameter bifurcation diagram as for I_{ext} showed that, the pacemaker rhythm changes sensitively to I_{ext}, and the action potential generation is accelerated by the external stimuli. In the two-parameter bifurcation diagrams as for c_{ion} and I_{ext}, it was shown that the interrelations between I_{Na} and I_{ext}, I_s and I_{ext}, I_K and I_{ext} are strong, whereas that between I_h and I_{ext} is weak. These results mean that the ion channels of I_{Na}, I_s, I_K are sensitive, whereas that of I_h is insensitive in both cases of a single cell and coupled cells. However, the cardiac muscle cells are stimulated by periodic electrical stimuli. The analysis of the YNI model with periodic stimuli or a model of coupled cells is necessary for more accurate information.

There are several limitations on the YNI model since it is an early and simple model. The YNI model does not consider some cellular functions such as exchangers and pumps, and all ionic concentrations are assumed to be constant. The sodium current I_{Na}, which corresponds to the Na^+ channel, changes with the region of sinoatrial node. The Na^+ channel is only present in the periphery cells of sinoatrial node (Zhang et al., 2000; Garny et al., 2003). Thus, it is necessary to analyze the effect of regional difference on pacemaker rhythm (Kurata et al., 2008). The slow inward current I_s plays an important role in action potential generation (Fig. 1), but it is a sum of the calcium current I_{Ca} and the sodium-calcium exchange current I_{NaCa} (DiFrancesco and Noble, 1985). Moreover, I_{Ca} can be divided into two types of currents: L-type and T-type calcium currents ($I_{Ca,L}$ and $I_{Ca,T}$), respectively. The potassium current I_K can also be divided into rapid and slow delayed rectifying potassium currents ($I_{K,r}$ and $I_{K,s}$) (Lei and Brown, 1996). Thus, it is necessary to analyze the effects of these ion channels or exchangers on pacemaker rhythm in detail.

In this paper, we only varied the conductances of ion channels and the external current as bifurcation parameters to analyze the dynamics of the YNI model (a HH-type model). However, for the HH-type models, their dynamics may change sensitively to various parameters, such as those in $\alpha_x(V)$ and $\alpha_x(V)$ of Eq. (7) (Doi et al., 2010; Csercsik et al., 2010; Bedrov et al., 1992, 1993). It is necessary to note that our results may change significantly with the variation of other parameters.

In conclusion, this paper have used a simple but typical cardiac pacemaker cell model for bifurcation analysis, and gained a rough sketch of the pacemaker rhythm. Therefore, the analysis of more detailed models and the comparison with these results are necessary as a future work.

Acknowledgments

This work was supported in part by the Global COE Program "in silico medicine" at Osaka University, the Kayamori Foundation of Informational Science Advancement, the Japan Society for the Promotion of Science, and the Aihara Project, the FIRST program from JSPS, initiated by CSTP. We would also like to thank all reviewers for their kind and useful comments to improve our manuscript much.

Appendix A.

$$\alpha_m(V) = \frac{V+37}{1-\exp(-((V+37)/10))}$$

$$\beta_m(V) = 40\,\exp\left(-\frac{V+62}{17.8}\right)$$

$$\alpha_h(V) = 1.209\times10^{-3}\exp\left(-\frac{V+20}{6.534}\right)$$

$$\beta_h(V) = \frac{1}{1+\exp(-((V+30)/10))}$$

$$\alpha_d(V) = \frac{1.045\times10^{-2}(V+35)}{1-\exp(-((V+35)/2.5))} + \frac{3.125\times10^{-2}V}{1-\exp(-(V/4.8))}$$

$$\beta_d(V) = \frac{-4.21\times10^{-3}(V-5)}{1-\exp((V-5)/2.5)}$$

$$\alpha_f(V) = \frac{-3.55\times10^{-4}(V+20)}{1-\exp((V+20)/5.633)}$$

$$\beta_f(V) = \frac{9.44\times10^{-4}(V+60)}{1+\exp(-((V+29.5)/4.16))}$$

$$\alpha_q(V) = \frac{-3.4\times10^{-4}(V+100)}{1-\exp((V+100)/4.4)} + 4.95\times10^{-5}$$

$$\beta_q(V) = \frac{5\times10^{-4}(V+40)}{1-\exp(-((V+40)/6))} + 8.45\times10^{-5}$$

$$\alpha_p(V) = \frac{9\times10^{-3}}{1+\exp(-((V+3.8)/9.71))} + 6\times10^{-4}$$

$$\beta_p(V) = \frac{-2.25\times10^{-4}(V+40)}{1-\exp((V+40)/13.3)}$$

References

Anon., 2007. http://www.lvma.org/rabbit.html.

Anumonwo, J., Wang, H., Trabka-Janik, E., Dunham, B., Veenstra, R., Delmar, M., Jalife, J., 1992. Gap junctional channels in adult mammalian sinus nodal cells: immunolocalization and electrophysiology. Circ. Res. 71, 229–239.

Barabási, A.L., Albert, R., 1999. Emergence of scaling in random networks. Science 286, 509–512.

Barbieri, R., Brown, E.N., 2008. Application of dynamic point process models to cardiovascular control. Biosystems 93, 120–125.

Bedrov, Y., Akoev, G., Dick, O., 1992. Partition of the Hodgkin–Huxley type model parameter space into the regions of qualitatively different solutions. Biol. Cybern. 66, 413–418.

Bedrov, Y., Akoev, G., Dick, O., 1993. Functional states of an excitable membrane and their dependence on its parameter values. Biol. Cybern. 70, 157–161.

Bowman, L.N., Jongsma, H.J., 1986. Structure and function of the sino-atrial node: a review. Eur. Heart J. 7, 94–104.

Brown, H.F., 1982. Electrophysiology of the sinoatrial node. Physiol. Rev. 62, 505–530.

Christen, J.A., Ruiz, G., Torres, J., 2001. Energy efficiency of information transmission by electrically coupled neurons. Biosystems 61, 27–32.

Csercsik, D., Farkas, I., Szederkényi, G., Hrabovszky, E., Liposits, Z., Hangos, K., 2010. Hodgkin–Huxley type modelling and parameter estimation of gnrh neurons. Biosystems 100, 198–207.

Di Bernardo, D., Signorini, M., Cerutti, S., 1998. A model of two nonlinear coupled oscillators for the study of heartbeat dynamics. Int. J. Bifurcat. Chaos 8, 1975–1985.

DiFrancesco, D., Noble, D., 1985. A model of cardiac electrical activity incorporating ionic pumps and concentration changes. Philos. Trans. R. Soc. Lond. B 307, 353–398.

Doedel, E.J., Champneys, A.R., Fairgrieve, T.F., Kuznetsov, Y.A., Sandstede, B., Wang, X., 1997. AUTO97: continuation and bifurcation software for ordinary differential equations (with HomCont). Technical Report. Concordia University.

Doi, S., Inoue, J., Pan, Z., Tsumoto, K., 2010. Computational Electrophysiology—Dynamical Systems and Bifurcations. Springer.

Dokos, S., Celler, B., Lovell, N., 1996. Ion currents underlying sinoatrial node pacemaker activity: a new single cell mathematical model. J. Theor. Biol. 181, 245–272.

Fink, M., Niederer, S., Cherry, E., Fenton, F., Koivumäki, J., Seemann, G., Thul, R., Zhang, H., Sachse, F., Beard, D., Crampin, E., Smith, N., 2011. Cardiac cell modelling: observations from the heart of the cardiac physiome project. Prog. Biophys. Mol. Biol. 104, 2–21.

Garny, A., Kohl, P., Hunter, P.J., Boyett, M.R., Noble, D., 2003. One-dimensional rabbit sinoatrial node models: benefits and limitations. J. Cardiovasc. Electrophysiol. 14, S121–132.

Gómez, L., Budelli, R., Pakdaman, K., 2001. Dynamical behavior of a pacemaker neuron model with fixed delay stimulation. Phys. Rev. E 64, 061910.

Guckenheimer, J., Holmes, P., 2002. Nonlinear Oscillations, Dynamical Systems, and Bifurcations of Vector Fields. Springer.

Hasegawa, H., 2000. Responses of a Hodgkin–Huxley neuron to various types of spike-train inputs. Phys. Rev. E 61, 718–726.

Hodgkin, A.L., Huxley, A.F., 1952. A quantitative description of membrane current and its application to conduction and excitation in nerve. J. Physiol. 117, 500–544.

Irisawa, H., Brown, H.F., Giles, W., 1993. Cardiac pacemaking in the sinoatrial node. Physiol. Rev. 73, 197–227.

Irisawa, H., Noma, A., 1982. Pacemaker mechanisms of rabbit sinoatrial node cells. In: Bouman, L.N., Jongsma, H.J. (Eds.), Cardiac Rate and Rhythm: Physiological, Morphological, and Developmental Aspects. Springer, pp. 35–51.

Jacquemet, V., 2006. Pacemaker activity resulting from the coupling with nonexcitable cells. Phys. Rev. E 74, 011908.

Joyner, R.W., Wilders, R., Wagner, M.B., 2006. Propagation of pacemaker activity. Med. Biol. Eng. Comput. 45, 177–187.

Keener, J., Sneyd, J., 2008. Mathematical Physiology II: Systems Physiology. Springer.

Kurata, Y., Hisatome, I., Imanishi, S., Shibamoto, T., 2002. Dynamical description of sinoatrial node pacemaking: improved mathematical model for primary pacemaker cell. Am. J. Physiol. Heart Circ. Physiol. 283, H2074–H2101.

Kurata, Y., Matsuda, H., Hisatome, I., Shibamoto, T., 2008. Regional difference in dynamical property of sinoatrial node pacemaking: role of Na^+ channel current. Biophys. J. 95, 951–977.

Lei, M., Brown, H.F., 1996. Two components of the delayed rectifier potassium current, I_K in rabbit sino-atrial node cells. Exp. Physiol. 81, 725–741.

Nagata, S., Takahashi, N., Doi, S., Kumagai, S., 2006. Analysis of stimulus response characteristics and drug sensitivity of ventricular myocardial cell using a nonlinear dynamic model. IEICE Trans. A J89-A, 1153–1167 (in Japanese).

Noble, D., 2002. Modeling the heart—from genes to cells to the whole organ. Science 1, 1678–1682.

Noble, D., Noble, S.J., 1984. A model of sino-atrial node electrical activity based on a modification of the DiFrancesco-Noble (1984) equations. Proc. R. Soc. Lond. B 222, 295–304.

Ozer, M., Perc, M., Uzuntarla, M., 2009. Stochastic resonance on newman-watts networks of Hodgkin–Huxley neurons with local periodic driving. Phys. Lett. 373, 964–968.

Perc, M., 2007. Stochastic resonance on excitable small-world networks via a pacemaker. Phys. Rev. E 76, 066203.

Perc, M., 2008. Stochastic resonance on weakly paced scale-free networks. Phys. Rev. E 78, 036105.

Perc, M., Gosak, M., 2008. Pacemaker-driven stochastic resonance on diffusive and complex networks of bistable oscillators. New J. Phys. 10, 053008.

Perc, M., Marhl, M., 2006. Pacemaker enhanced noise-induced synchrony in cellular arrays. Phys. Lett. A 353, 372–377.

Sarai, N., Matsuoka, S., Kuratomi, S., Ono, K., Noma, A., 2003. Role of individual ionic current systems in the sa node hypothesized by a model study. Jpn. J. Physiol. 53, 125–134.

Sato, S., Nomura, T., Doi, S., Yamanobe, T., 1997. On the behavior of mRIC—a simple model of living pacemakers driven by periodic pulse trains. Biosystems 40, 169–176.

Takahashi, N., Doi, S., Kumagai, S., 2006. Parameter estimation of ventricular myocardial cell model using an on-line learning algorithm. In: Proc. SICE-ICCAS International Joint Conference 2006 , pp. 2322–2327.

Torrealdea, F.J., d'Anjou, A., Graña, M., 2006. Energy aspects of the synchronization of model neurons. Phys. Rev. E 74, 011905.

Torrealdea, F.J., Sarasola, C., d'Anjou, A., Moujahid, A., de Mendizábal, N., 2009. Energy efficiency of information transmission by electrically coupled neurons. Biosystems 97, 60–71.

Van Rijen, H.V.M., Wilders, R., Van Ginneken, A.C.G., Jongsma, H.J., 1998. Quantitative analysis of dual whole-cell voltage-clamp determination of gap junctional conductance. Pflug. Arch. Eur. J. Phys. 436, 141–151.

Verheule, S., Van Kempen, M., Postma, S., Rook, M., Jongsma, H., 2001. Gap junctions in the rabbit sinoatrial node. Am. J. Physiol. Heart Circ. Physiol. J89-A, H2103–H2115.

Wahler, G.M., 2001. Cardiac action potentials. In: Sperelakis, N., Kurachi, Y., Terzic, A., Cohen, M. (Eds.), Heart Physiology and Pathophysiology. , fourth edition. Academic Press, pp. 199–211.

Watts, D.J., Strogatz, S.H., 1998. Collective dynamics of 'small-world' networks. Nature 393, 440–442.

Wilders, R., 2007. Computer modelling of the sinoatrial node. Med. Biol. Eng. Comput. 45, 189–207.

Wilders, R., Jongsma, H.J., Ginneken, A.C.G., 1991. Pacemaker activity of the rabbit sinoatrial node: a comparison of mathematical models. Biophys. J. 60, 1202–1216.

Yamaguchi, R., Doi, S., Kumagai, S., 2007. Bifurcation analysis of a detailed cardiac cell model and drug sensitivity of ionic channels. In: Proc. 15th IEEE International Workshop on Nonlinear Dynamics of Electronic Systems 2007 , pp. 205–208.

Yamaguchi, R., Hisakado, S., Doi, S., 2008. Comprehensive bifurcation analysis of cardiac cell models. In: Proc. Second China-Japan Colloquium of Mathematical Biology.

Yamanobe, T., Pakdaman, K., 2002. Response of a pacemaker neuron model to stochastic pulse trains. Biol. Cybern. 86, 155–166.

Yamanobe, T., Pakdaman, K., Nomura, T., Sato, S., 1998. Analysis of the response of a pacemaker neuron model to transient inputs. Biosystems 48, 287–295.
Yanagihara, K., Noma, A., Irisawa, H., 1980. Reconstruction of sinoatrial node pacemaker potential based on the voltage clamp experiments. Jpn. J. Physiol. 30, 841–857.
Zhang, H., Holden, A.V., Kodama, I., Honjo, H., Lei, M., Varghese, T., Boyett, M.R., 2000. Mathematical models of action potentials in the periphery and center of the rabbit sinoatrial node. Am. J. Physiol. Heart Circ. Physiol. 279, H397–H421.